Research Paper

EARTHQUAKE SPECTRA

Earthquake Spectra
1–25

DOI: 10.1177/87552930251350158
journals.sagepub.com/home/eqs
Sage

Derivation of fragility curves to assess and compare the effectiveness of retrofitting strategies in URM buildings

Stefania Degli Abbati, M. EERI, Andrea Brunelli, Arash Rooshenas, and Sergio Lagomarsino

Abstract

Recent earthquakes have highlighted the seismic vulnerability of existing masonry buildings, pointing out the urgent need to design high-performance and non-invasive strengthening interventions. To this aim, reliable numerical models and assessment procedures are necessary to evaluate their effectiveness and quantify the effects on the structural seismic performance of the building. In this context, the article describes a procedure for the seismic assessment of existing masonry buildings and the design of retrofitting strategies. The procedure is based on a suitable nonlinear numerical model and consists of three phases. In the first phase, the numerical model is defined. In the second phase, the seismic assessment of the building in the as-built configuration is performed, and the required strengthening interventions are designed using nonlinear static analyses. In the third phase, the actual effects of the proposed interventions are evaluated through nonlinear dynamic analyses and the derivation of fragility curves. To test its reliability, the article describes the application of the procedure to two case studies representative of ordinary unreinforced masonry buildings placed in Italy and considered both in the as-built and retrofitted configurations. Their seismic performance was assessed through several nonlinear dynamic analyses performed according to the multiple-stripe approach and employing an equivalent frame modeling strategy. Different strengthening techniques were investigated, designed to conform with the Italian Technical Code, and modulated to achieve a safety index higher than 1 or 0.8 (allowed by the code for existing buildings) as a function of two different site categories (stiff and soft soils). The resulting fragility curves were used to quantify the improvement of the seismic performance guaranteed by the different strengthening strategies and compare their effectiveness concerning two

DICCA, Department of Civil, Chemical and Environmental Engineering, University of Genoa, Genoa, Italy

Corresponding author:
Stefania Degli Abbati, DICCA, Department of Civil, Chemical and Environmental Engineering, University of Genoa, Via Montallegro 1, Genoa 16145, Italy.
Email: stefania.degliabbati@unige.it

performance conditions (namely usability-preventing damage and global collapse limit states) to identify the best solution for the two considered site categories.

Keywords
Retrofitting, masonry, pushover analyses, nonlinear dynamic analyses, fragility curves

Date received: 4 November 2024; accepted: 23 April 2025

Introduction

Existing unreinforced masonry (URM) buildings have consistently shown poor performance during past seismic events, including the Umbria-Marche 1997 earthquake (Spence and D'Ayala, 1999), the L'Aquila 2009 earthquake (Augenti and Parisi, 2010; D'Ayala and Paganoni, 2011), the Emilia 2012 earthquake (Cattari et al., 2012; Penna et al., 2014), and the Central Italy 2016 earthquake (Sorrentino et al., 2019). To mitigate the seismic vulnerability of URM buildings, it is crucial to design high-performance, non-invasive strengthening interventions. Several seismic upgrading techniques are available for URM structures (Gkournelos et al., 2022), whose effectiveness must be assessed through numerical models and evaluation procedures that can accurately quantify their impact on structural performance. However, the implementation of some strengthening interventions into numerical models can be challenging. Due to software limitations or the assumptions inherent in the chosen modeling strategies, the numerical model is not always able to accurately assess the actual effects of the selected retrofitting solutions and reliably predict the enhanced seismic performance of structures. In addition, while modern seismic design standards focus on the safety of new buildings, standards and guidelines for retrofitting existing structures are relatively recent. As a result, there are no widely established procedures for designing strengthening interventions and verifying their effects on building response.

Linear analyses or methods based on local stress-state verification often provide overly simplistic assessments for URM buildings. Therefore, nonlinear analysis procedures are essential for obtaining more reliable results. Two primary options are available: nonlinear dynamic analysis (NLDA) and nonlinear static analysis (NLSA). NLDA represents the most advanced analysis method currently available. However, it is computationally demanding and presents several challenges:

- Few numerical models can perform time-history analyses for URM structures, largely due to the complexity of defining cyclic constitutive and viscous damping models (Mouyiannou et al., 2014).
- The selection of appropriate accelerograms can significantly affect the structural response and the results, particularly due to record-to-record variability, which is exacerbated when a limited number of records is used, as suggested by building codes (Jalayer et al., 2021).
- Safety assessment procedures for designing strengthening interventions in dynamic analyses of URM buildings are still under development.
- Interpreting the large number of results generated by NLDA is complex, but it is an indispensable tool for designing effective strengthening interventions.

For these reasons, NLSA is the method typically prescribed by Codes and widely used by practitioners to assess the seismic performance of existing URM buildings in their as-built

condition, design appropriate retrofitting solutions, and evaluate their safety in the retrofitted state. While Marino et al. (2019) provide a review of NLSA's reliability when applied to regular and irregular URM buildings, a validation of its ability to predict the actual improvements achieved through strengthening interventions still lacks in the literature.

In this context, this article proposes a procedure for deriving fragility curves (Section "Adopted procedure for the seismic assessment and the design of strengthening interventions") to assess the seismic performance of existing URM buildings in both their as-built and retrofitted conditions and applies it to two selected case studies (Sections "Application of the procedure to BLDG 1" and "Application of the procedure to BLDG 2"). A detailed description of the two case studies is provided in Section "Description of the selected case studies." The procedure is divided into three phases (Figure 1). In the first phase, a modeling strategy is selected, and a three-dimensional (3D) numerical model is created to replicate the geometry and mechanical properties of the building. Next, in the second phase, the building's seismic performance is evaluated, and potential strengthening interventions are designed using code-base procedures, prescriptions, and tools prescribed by Standards (including NLSAs, constitutive law, and drift values). Finally, in the third phase, the seismic assessment is carried out with NLDA and fragility curves, employing more advanced constitutive laws and assumptions for the numerical model.

It should be noted that the activities presented in this article are part of a research project started in 2015 (Iervolino et al., 2023b) and conducted under the ReLUIS (Rete dei Laboratori Universitari di Ingegneria Sismica) Consortium. This consortium is an inter-university network supported by the Italian Civil Protection, aiming to coordinate research efforts in Earthquake and Structural Engineering across the scientific community.

Adopted procedure for the seismic assessment and the design of strengthening interventions

This section outlines the procedure proposed by the authors to assess and compare the effectiveness of retrofitting strategies through the derivation of fragility curves. Figure 1 illustrates the five steps of the proposed methodology and its main goals.

The first step (i.e. the *"modeling" phase*) involves setting up a 3D numerical model of the building, capable of capturing its nonlinear response. Among various modeling strategies (D'Altri et al., 2020), this article employs the equivalent frame (EF) modeling approach as implemented in the 3muri software, distributed by S.T.A DATA (Lagomarsino et al., 2013). In the EF model, only the in-plane behavior of masonry walls is considered, with deformability and nonlinear behavior concentrated into specific portions of URM walls: the piers (vertical elements) and spandrels (masonry beams connecting two adjacent piers). Piers and spandrels are connected through rigid areas (nodes). The EF approach is reliable if a box-like behavior is ensured. In 3muri, the structural elements are modeled as nonlinear bidimensional beams, following a bilinear elastic-perfectly plastic constitutive law, with limits on maximum (ultimate) displacement and stiffness degradation in the nonlinear range. Failure modes under horizontal forces include flexural-rocking, shear-sliding, and diagonal shear cracking. Collapse occurs when the panel reaches its ultimate drift capacity, specific to each failure mode. According to the provisions of the Italian Technical Code (NTC, 2018 and MIT, 2019) and Eurocode 8 (CEN EN 1998-1, 2004), ultimate drift values are specified for piers and spandrels. In the examined case, following the Italian Code's suggestions, the values of piers are set at 0.5% and

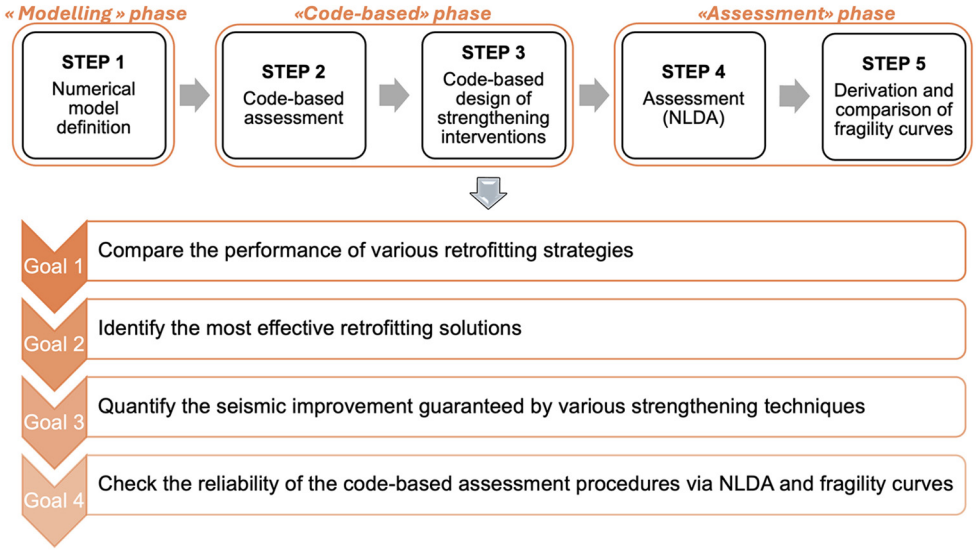

Figure 1. The three phases and five steps of the methodology.

1% (for shear failure or flexural failure, respectively). In comparison, the values of spandrels are 1.5% (for shear failure and flexural failure). If spandrels are coupled with tensile-resistant elements, the drift for flexural failure is 2%.

The next step (Step 2 in Figure 1) involves a code-based assessment of the building in its as-built configuration to determine whether its seismic performance is adequate or needs improvement. According to current methods prescribed by Technical Codes and Standards, the seismic assessment of existing URM buildings is conducted using NLSA, applying at least two different load patterns. For instance, MIT (2019) specifies two load patterns: one proportional to the masses and another proportional to the product of the mass matrix, and the first mode shape, assumed to be linear along the height. As an output of NLSA, a pushover curve representing the behavior of the multi-degree-of-freedom system (MDOF) is obtained for each load pattern and analysis. This pushover curve is then transformed into the capacity curve of an equivalent single-degree-of-freedom (SDOF) system and compared with the acceleration-displacement response spectrum (ADRS) to evaluate the seismic demand corresponding to the achievement of the selected performance levels (a_{LS}). Several methods have been proposed in the literature to appropriately reduce the elastic spectrum before comparing it with the capacity curve of the SDOF system. These include the Coefficient Method (ASCE/SEI 41-23, 2023), the N2 Method (Fajfar, 1999), and the Capacity Spectrum Method (Freeman, 1998). To quantify building performance, a safety index α can be calculated as the ratio between the maximum acceleration corresponding to the attainment of the considered limit state (a_{LS}) and the peak ground acceleration at the site ($a_{g,LS}$). Safety indices lower than unity indicate a higher likelihood of significant damage and the need for retrofitting interventions.

The third step of the proposed procedure is the code-based design of retrofitting interventions, using NLSA and the same verification methodology described in the previous step. Various strengthening measures are tailored to achieve a safety index greater than 1, or 0.8 (as permitted by MIT, 2019, for existing buildings), depending on two different site

categories, hereafter referred to as stiff and soft soils. This approach enables the authors to explore both highly effective but more invasive retrofitting options as well as lighter, less intrusive solutions.

Steps 2 and 3 belong to the "*code-based phase*".

The final two steps of the procedure, referred to as the *"assessment phase,"* aim to evaluate the actual effects of the strengthening interventions designed in Step 3 on the building's seismic response using fragility curves derived from NLDA. For this purpose, in this article, the nonlinear response of panels was modeled using the piecewise-linear constitutive laws formulated by Cattari and Lagomarsino (2013) and implemented in the research version of the Tremuri software package (Lagomarsino et al., 2013). This constitutive law proposed by Cattari and Lagomarsino (2013) is based on a phenomenological approach and better represents the actual nonlinear behavior of existing URM buildings, even at severe damage levels (DL, from 1 to 5). It captures progressive stiffness and strength degradation at specified drift values. The model requires the definition of parameters that describe the progression of the nonlinear response as damage levels increase, differentiated for piers, spandrels, and flexural and shear behavior. The hysteretic response is governed by a set of parameters that control the slopes of the loading and unloading branches. The parameters required to define the constitutive law used in this article are described in detail in Sections "Application of the procedure to BLDG 1" and "Application of the procedure to BLDG 2."

The NLDAs were conducted using the multiple-stripe approach (MSA, see Lin et al., 2013), which involves selecting various sets of accelerograms for each intensity measure level (*"stripes"*). The accelerations in each stripe are chosen to represent the seismic scenario associated with that level of shaking at the site, as determined by seismic hazard disaggregation. In this case, each stripe includes 20 seismic records representing the seismicity of L'Aquila. These records are conditioned to the first-mode structural acceleration, which is assumed to be the intensity measure (IM). The records were selected for buildings with a fundamental period of 0.15 s (for BLDG 1) and 0.5 s (for BLDG 2), and for two site categories (stiff and soft). Each set of accelerograms is spectrum-compatible with 10 increasing values of return periods: 10 years for IM of stripe 1, 50 for stripe 2, 100 for stripe 3, 250 for stripe 4, 500 for stripe 5, 1000 for stripe 6, 2500 for stripe 7, 5000 for stripe 8, 10,000 for stripe 9, and 100,000 for stripe 10. The selection criteria for the seismic records are described in detail by Iervolino et al. (2018).

Two different performance states were considered, global collapse (GC) and usability-preventing damage (UPD), within a framework like that used in Iervolino et al. (2023a). The capacity for these performance states was identified by the maximum inter-story drift ratio (among all walls and all stories), considered the key engineering demand parameter (EDP). The thresholds for GC and UPD were defined as follows: the GC thresholds were established through uniform NLSA in both directions (X and Y) and for both positive and negative loading, corresponding to a 50% post-peak reduction in total base shear. The UPD thresholds were defined as the more conservative of two conditions in the NLDA: either the first pier reaching damage level DL3, or 50% of piers reaching DL2, according to the constitutive law proposed by Lagomarsino and Cattari (2015). The definition of the performance states is coherent with those specified in international codes. The GC should be considered beyond the near-collapse limit state because the residual lateral strength and stiffness, as well as the capacity to gravity loads, remain very limited. In contrast, the UPD is similar to the damage limitation limit state of Eurocode 8 and the immediate occupancy

in ASCE/SEI 41–23, because the building retains its structural integrity, ensuring sufficient residual load-bearing capacity.

To demonstrate the actual effects of the interventions designed according to code procedures, fragility curves were derived for each limit state, both for the as-built and retrofitted configurations, using the R2R software (Baraschino et al., 2020; Iervolino, 2017) and based on the results of the NLDA. Basically, the effectiveness is ensured if the fragility curve shifts to the right compared to the as-built condition. To quantify the improvement induced by the interventions, the probability of exceeding the limit state is computed by intersecting the curves with the IM associated with a specific return period. The greater the decrease in the probability of reaching the limit state in the retrofitted configurations, the more effective the intervention is in improving structural performance. Analogously, a reference probability of failure might be selected and the corresponding IM values before and after the intervention may be compared. The comparison of these fragility curves allowed the authors to: (1) Compare the performance of the various selected retrofitting strategies, (2) Identify the most effective strengthening interventions, (3) Quantify the seismic improvements provided by the different retrofitting solutions, and (4) Evaluate the reliability of current code-based assessment procedures used by practitioners to predict the improved behavior, using NLDA and fragility curves as benchmarks.

Description of the selected case studies

This section summarizes the main features of the two selected case studies. While inspired by real structures, their as-built configurations and mechanical properties have been intentionally modified to increase their vulnerability. This modification allows the authors to design a range of strengthening interventions (with increasing performance) and assess their impact on the structural response, thereby demonstrating the effectiveness of the procedure introduced in Section "Adopted procedure for the seismic assessment and the design of strengthening interventions."

The first case study, referred to as BLDG 1, is a 3-story URM building with a regular layout in both plan and elevation. The building has plan dimensions of 20.5×12.7 m, with inter-story heights of 3.8 m for the first two levels and 4.7 m for the top level. The case study is modeled after a historical residential building constructed in the 1920s in Norcia, Italy, but analyzed with the seismic characteristics of L'Aquila. The external and internal walls of the first two stories have thicknesses of 0.8 and 0.6 m, respectively. In contrast, the walls on the third level vary in thickness from 0.25 to 0.6 m. The masonry of the first two floors consists of irregular stones, while the internal walls of the third level are made of solid bricks and lime mortar. Openings are vertically aligned, measuring approximately 1.5 m on the first two floors and about 2.05 m on the upper floor. The building features barrel and cross vaults on the ground floor and relatively thin barrel vaults (0.25 m thick at the keystone) on the upper floors. Figure 2a shows a picture of the actual building and the simplified geometrical scheme used for the various floors. Further details can be found in Lagomarsino et al. (2023).

The second case study, referred to as BLDG 2, is a 3-story URM building inspired by the Pizzoli town hall (Figure 2b), which was hit by the 2016–2017 Central Italy earthquake (Degli Abbati et al., 2022a). Some simplifications were made for the as-built configuration, including the addition of a third story. BLDG 2 features a regular elevation and a C-shaped floor plan, with dimensions approximately 38×12.5 m (Figure 2b). It has three levels, a basement (which is neglected in the model), and a non-habitable attic (modeled as

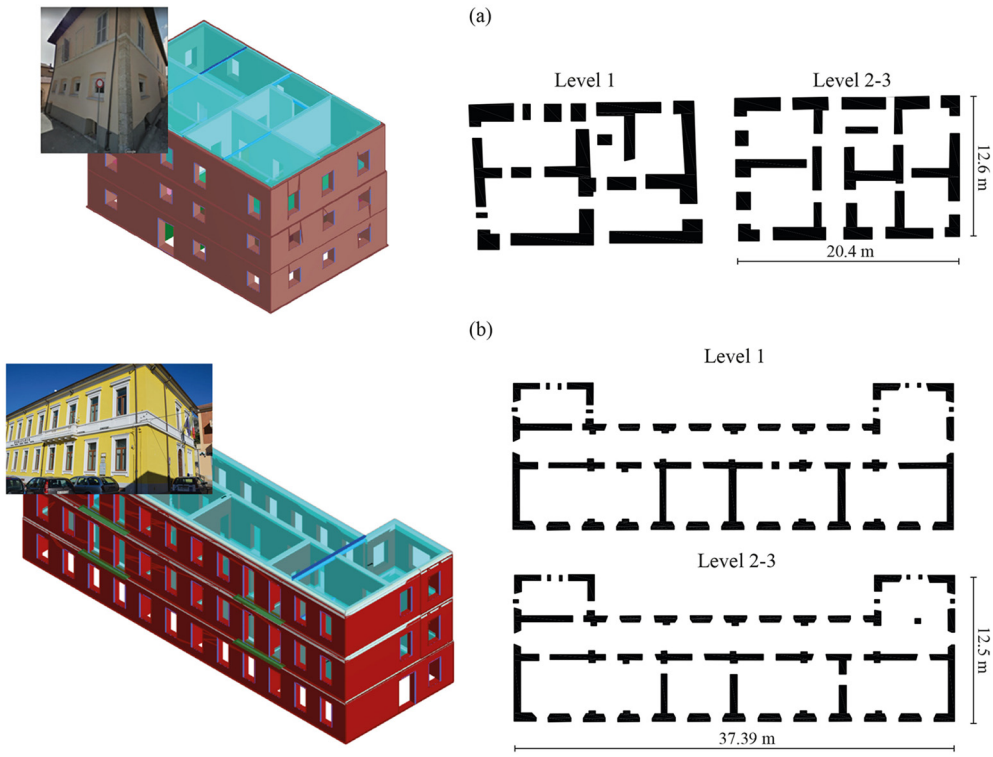

Figure 2. Pictures, 3D models, and plans of the buildings which inspired the two examined case studies: (a) residential building in Norcia (BLDG 1) and (b) the Pizzoli's town hall (BLDG 2).

Table 1. Mechanical properties assumed for the two case studies

Case study	Masonry type	f_m [N/cm^2]	τ_0 [N/cm^2]	E [N/mm^2]	G [N/mm^2]	w [kN/m^3]
BLDG 1	Irregular stone masonry	150	2.5	870	290	19
	Brick masonry	448.5	11.7	1500	500	18
BLDG 2	Regular stone masonry	300	6.45	1230	410	20

an equivalent load). The attic is characterized by a pavilion roof made up of reinforced concrete (RC) joists and hollow clay units, with a 3-cm-thick slab. The total height of the building is approximately 13 m. The walls are made of regular stone masonry, and the floors consist of a small iron beam and hollow-clay-block floor system, topped with an RC slab.

Table 1 presents the mechanical properties used in the numerical models of the two case studies. These properties include mean masonry compressive strength (f_m), masonry shear strength (τ_0), masonry elastic modulus (E), masonry shear modulus (G), and masonry specific weight (w). The selected values are based on the recommendations outlined in MIT (2019). The masonry elastic moduli refer to the initial elastic condition. To represent a cracked condition, the elastic parameters were divided by two, in line with typical code suggestions and experimental data (e.g. Vanin et al., 2017). It should be noted that

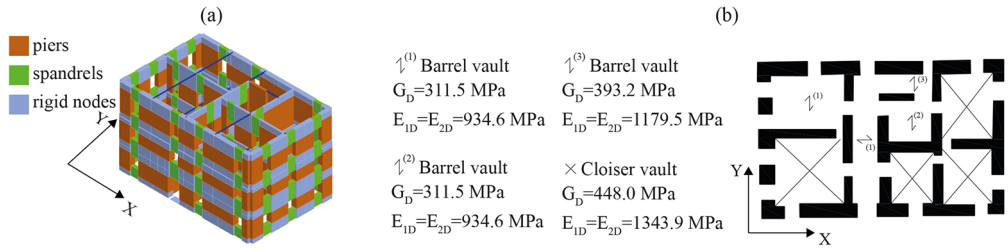

Figure 3. (a) 3D view of the EF numerical model of BLDG1 and (b) floor plan of the building.

different mechanical parameters were assumed for the stone masonry in the two case studies to account for the varying typologies and quality observed on-site in each building. Specifically, for BLDG 1, the mean values of the range proposed by MIT (2019) for rubble stone masonry were used as a reference. In contrast, for BLDG 2, starting from the mean values suggested by MIT (2019) for more regular stone masonry, a corrective coefficient $k_1 = 1.5$ was applied solely to the strength parameters to account for effective cross-connection. Finally, for the brick masonry in BLDG 1, the mean values within the range proposed by MIT (2019) were adopted, with strength parameters multiplied by $k_2 = 1.3$ to account for good interconnection among the masonry leaves.

Application of the procedure to BLDG 1

This section illustrates the application of the proposed procedure described in Section "Adopted procedure for the seismic assessment and the design of strengthening interventions" to the first case study, which is the 3-story URM building inspired by the residential building in Norcia (BLDG 1).

Code-based assessment of the as-built configuration and design of retrofit interventions

Figure 3 shows the 3D EF numerical model of the building, developed using the available data on geometry, materials, and structural details (Section "Description of the selected case studies"). All URM walls were idealized as equivalent frames, consisting of masonry panels modeled as piers and spandrels, connected by rigid nodes (Figure 3a). Among the various criteria proposed in the literature for mesh geometry definition (Augenti, 2006; Dolce, 1991; Lagomarsino et al., 2013; Moon et al., 2006), the 3Muri software automatically applies the criteria suggested by Lagomarsino et al., 2013. This approach has been validated by various research studies and is considered reliable when the layout of openings is relatively regular (Cattari et al., 2021; Ottonelli et al., 2021). Once the 2D modeling of the walls was completed, it was used to construct the entire 3D model by incorporating the diaphragms. In 3Muri, diaphragms are modeled as 3- or 4-node finite orthotropic membrane elements, characterized by the Young's modulus E_{1D} along the principal direction (corresponding to the floor span), the Young modulus E_{2D} along the perpendicular direction, the Poisson's ratio v, and the shear modulus G_D. Figure 3b shows the data of the floors assumed for BLDG 1.

After setting up the EF model, NLSAs were conducted, considering both the as-built and retrofitted configurations of the building. Two different load patterns were applied:

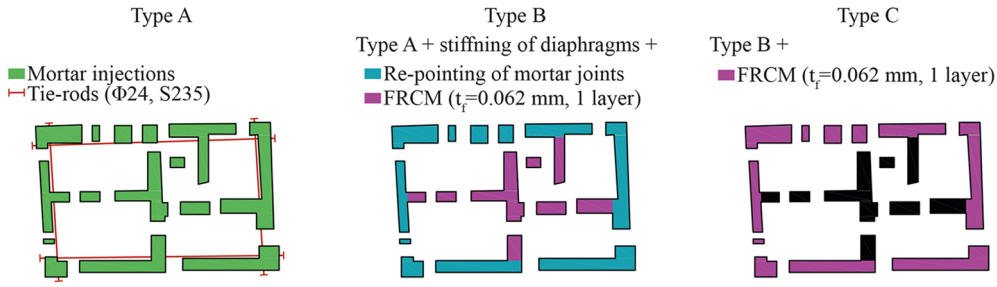

Figure 4. Interventions designed for BLDG 1 identified on the plan.

one proportional to masses (hereinafter named "Uniform") and one proportional to the product of the mass matrix time the first mode shape, considered linear along the height (hereinafter named "Static Force"). Various strengthening interventions were designed to comply with the Italian technical code (NTC, 2018) and modulated to achieve a safety index (α) higher than 1, or 0.8, as allowed by the code for existing buildings, depending on two different site categories—stiff and soft soils.

The three types of interventions designed were:

- Type A intervention: this intervention involves mortar injections into all masonry piers and a tie-rod (Φ24, steel S235) in the perimeter walls. With Type A intervention, the safety index for the L'Aquila site with stiff soil is higher than 0.8.
- Type B intervention: this includes all the strengthening measures from Type A, plus additional enhancements: stiffening of the diaphragms using FRCM (Fiber Reinforced Cementitious Matrix), re-pointing of mortar joints in the perimeter walls in the most critical direction, and the addition of one layer of FRCM (thickness $t_f = 0.062$ mm, tensile modulus of elasticity $E_f = 60{,}000$ GPa, ultimate deformation $\varepsilon_{fk} = 3\%$) to both faces of the internal walls. Type B intervention achieves a safety index higher than 1 in all NLSA for stiff soil and higher than 0.8 for soft soil.
- Type C intervention: this encompasses all measures from Type B but extends the application of FRCM to all walls in the building. This approach results in a safety index higher than 1 in all analyses, even for the building on soft soil.

The localization of these interventions is shown in Figure 4.

In terms of the modeling strategies used for the strengthening interventions, mortar injections and re-pointing of mortar joints are simulated by increasing both the strength (f_m, τ_0) and stiffness (E, G) parameters of the masonry, without altering the ultimate drift conditions, in line with the guidelines of MIT (2019). The stiffening of diaphragms is modeled by increasing the in-plane stiffness of the equivalent orthotropic membranes while maintaining the mass of the vaults to simulate an intervention with FRCM. In addition, the perimeter tie-rods introduced in the Type A intervention are explicitly represented in the numerical model as tensile-resistant elements to enhance the performance of the spandrels. Finally, for the Type B and Type C interventions, the FRCM applied to the masonry walls is modeled by increasing the shear strength and drift thresholds, following the guidelines of CNR-DT 215/2018 (2018) as described more in detail in Section "Results of the seismic assessment."

Table 2. Summary of the strengthening interventions designed for BLDG 1 according to NTC (2018)

Site category	Objective 1 $\alpha>0.8$	Objective 2 $\alpha>1$
Stiff soil	Type A intervention	Type B intervention
Soft soil	Type B intervention	Type C intervention

Table 3. Summary of safety indexes obtained for BLDG 1 from the NLSA for the as-built and retrofitted configurations for different load patterns and soil conditions (stiff and soft)

Site category		As-built		Type A intervention		Type B intervention	
Stiff soil		Min	Max	Min	Max	Min	Max
	Uniform X	0.69	0.86	1.11	1.19	1.30	1.39
	Static Force X	0.93	0.97	1.22	1.29	1.46	1.53
	Uniform Y	0.84	0.90	1.18	1.65	1.58	1.72
	Static Force Y	0.73	0.83	0.84	1.00	1.05	1.29
		Min	Max	Min	Max	Min	Max
Soft soil		As-built		Type B intervention		Type C intervention	
	Uniform X	0.46	0.55	0.81	0.86	1.40	1.48
	Static Force X	0.59	0.66	1.11	1.21	1.26	1.87
	Uniform Y	0.63	0.79	1.14	1.30	1.31	1.48
	Static Force Y	0.50	0.59	0.80	0.90	1.00	1.08

The color legend indicates whether α is higher than 1 (green), higher than 0.8 (orange), or lower than 0.8 (red).

Table 2 summarizes the strengthening interventions designed according to NTC (2018), while Table 3 presents the safety indexes (α) as obtained from the NLSA. Specifically, the table includes the minimum and maximum values for different load distribution patterns (i.e. proportional to masses and proportional to the product of masses and heights) across various configurations (current state and different retrofitting scenarios) and soil types (stiff or soft). The color legend indicates whether α is higher than 1 (green), higher than 0.8 (orange), or lower than 0.8 (red). Note that these safety indexes refer to the near-collapse limit state as defined by NTC (2018) (PGA = 0.33g for stiff soil and PGA = 0.41g for soft soil).

Figure 5 shows the 24 pushover curves obtained from the NLSA performed with the 3muri software in the code-based assessment phase. The graphs reveal that the Y-direction is more vulnerable, showing a lower maximum base shear across all examined configurations. In addition, the designed strengthening interventions enhance strength and stiffness, with the elastic first period moving from 0.28 s in the as-built configuration to a range of 0.24–0.22 s in the retrofitted configurations (these values were obtained from the modal analysis). Furthermore, Type B and Type C interventions also increase the maximum displacement capacity, thanks to the inclusion of FRCM strengthening measures.

Results of the seismic assessment

To assess the actual effects of the strengthening interventions described in Section "Code-based assessment of the as-built configuration and design of retrofit interventions," the research version Tremuri of the commercial software 3muri was used to perform NLDA

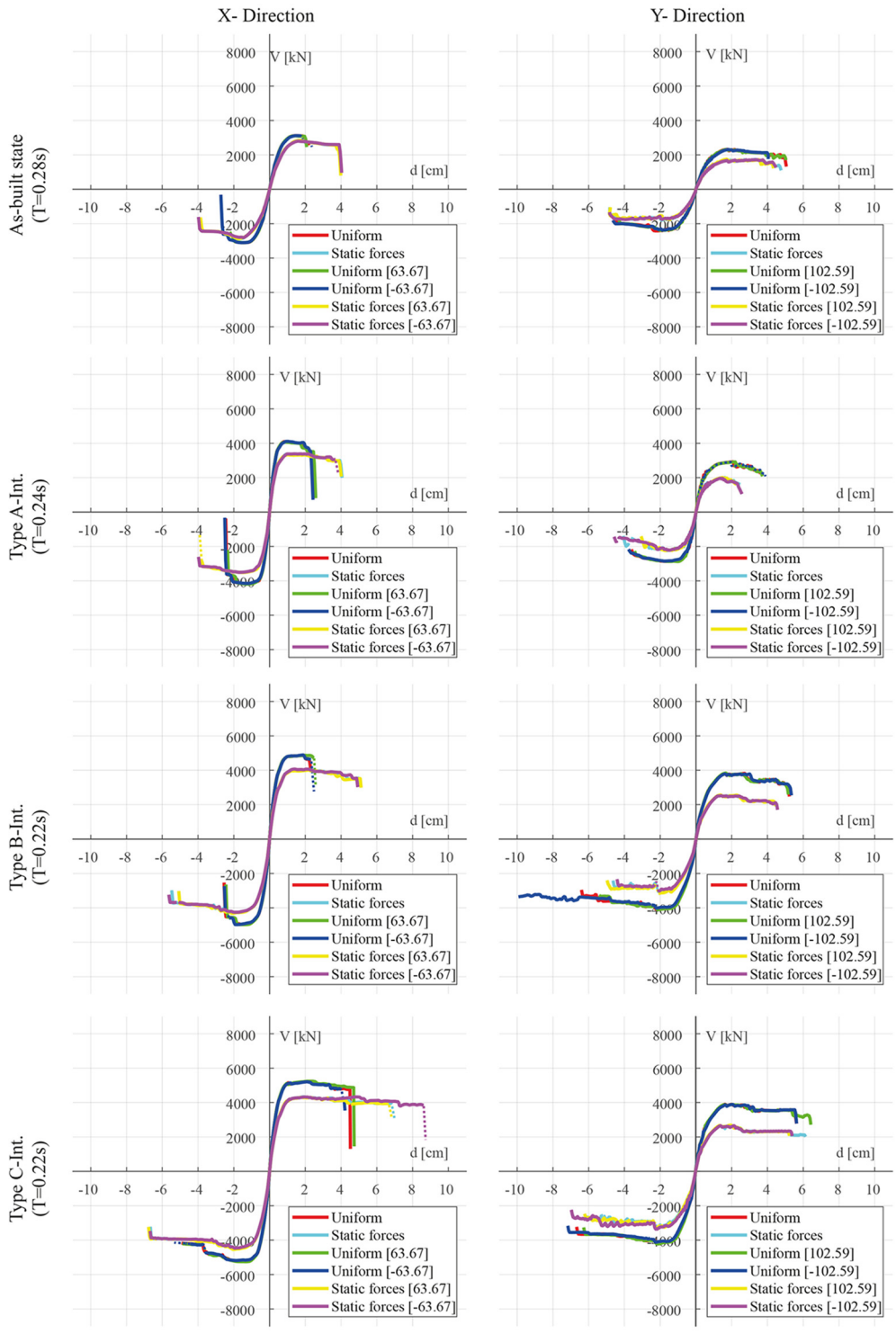

Figure 5. Pushover curves obtained from the NLSA with the 3muri software: as-built configuration and different strengthening interventions designed for BLDG 1.

Table 4. Parameters adopted for piers and spandrels (in brackets) in the piece-wise linear constitutive law for BLDG 1

	SHEAR		*FLEXURAL*	
	Drift [%]	Residual strength [%]	Drift [%]	Residual strength [%]
DL3	0.40 (*)	60 (40)	0.60 (0.60)	100 (100)
DL4	0.45 (0.40)	10 (40)	1.40 (0.80)	80 (40)
DL5	0.70 (0.70)	0 (0)	2.00 (1.20)	0 (0)

*Defined starting from drift corresponding to the yielding point of the element and assuming a ductility factor equal to 4.

on the EF model. These analyses employed the piecewise-linear constitutive laws formulated by Cattari and Lagomarsino (2013), as detailed in Section "Adopted procedure for the seismic assessment and the design of strengthening interventions." The parameters required for this law are presented in Table 4. The drift for DL3 of the spandrels was determined based on the drift corresponding to the yielding point of the element, with a ductility factor set to 4, following the approach suggested by Beyer and Mangalathu (2014).

It should be noted that current standards, including NTC (2018), prescribe the same drift limits regardless of the masonry typology, whether for as-built or retrofitted configurations. Thus, the latter values are those used for code-based assessments and during the design phase. However, for interventions with FRCM, an increased drift value has been assumed, calculated following CNR-DT 215/2018 (2018) (for piers: $\text{drift}_{\text{shear}} = 0.6\%$ and $\text{drift}_{\text{flexural}} = 1.2\%$, obtained by multiplying the initial values by 1.3). According to CNR-DT 215/2018 (2018), the shear capacity of the strengthened wall is calculated as the sum of the contribution of the URM panel, evaluated according to the formulation of codes for a masonry element failure, and the contribution of the reinforcement. The latter depends on the number of reinforcement layers applied to the faces of the wall, the equivalent thickness of fiber layers oriented parallel to the shear force, and the size of the reinforcement measured orthogonally to the shear force.

Figure 6 shows the inter-story drifts $\theta_{\max}$ (indicated on the Y-axis of the graphs) derived from the NLDA results of the MSA using spectrum-compatible ground motion records. These results are presented for the Y-direction only and both stiff and soft soils, comparing the as-built configuration with the two retrofitted scenarios. The round markers represent the maximum inter-story drift caused by the 20 records within each of the 10 stripes (on the X-axis), as described in Section "Adopted procedure for the seismic assessment and the design of strengthening interventions," while the dashed line indicates the mean value calculated excluding certain collapses, as reported in the round brackets. For the NLDA, it is assumed a certain collapse occurs when the value of the displacement induced by the accelerograms corresponds to an almost zero base shear (95% reduction). The red horizontal line denotes the GC threshold. When the inter-story drift exceeds this threshold, it means that the GC performance state is reached. Figure 6 shows a significant dispersion in the dynamic results, which can be attributed to record-to-record variability. However, when comparing the as-built state with the retrofitted configurations, both the GC threshold and the mean inter-story drifts are observed to increase. This suggests that the GC is induced in the retrofitted building by records from higher stripes, which correspond to higher return periods. A similar effect has also been observed in the X-direction.

Figure 7 illustrates the fragility curves computed with the R2R software (Baraschino et al., 2020; Iervolino, 2017) for the building on both stiff (Figure 7a) and soft soils (Figure

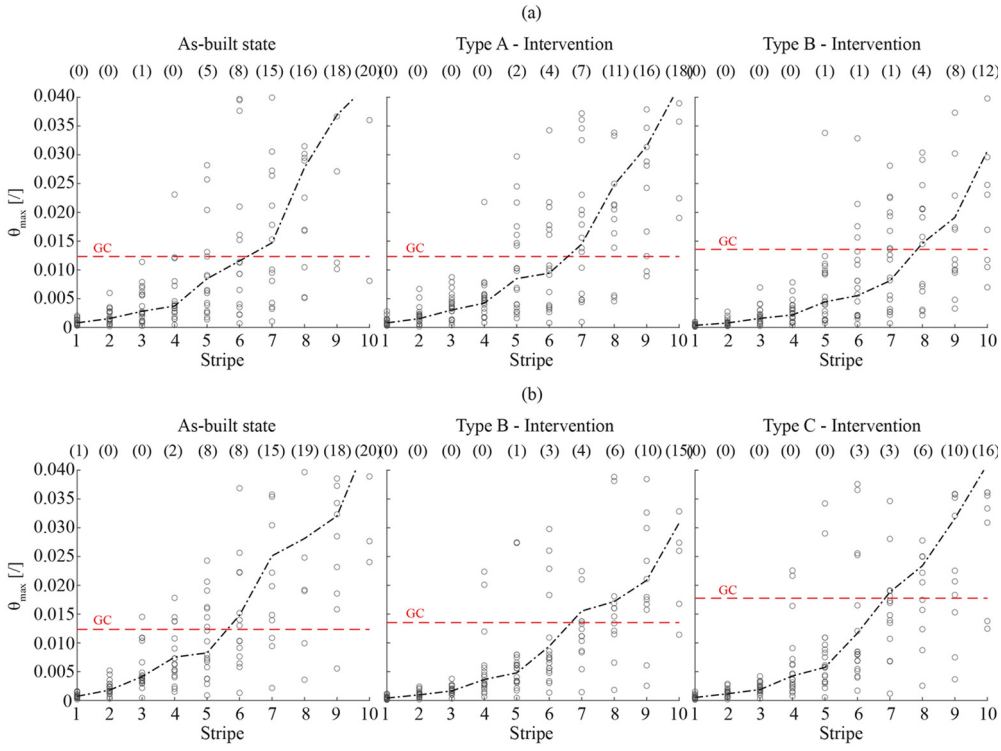

Figure 6. Inter-story drifts obtained by NLDA for the 10 stripes and Y-direction: (a) stiff soil and (b) soft soil.

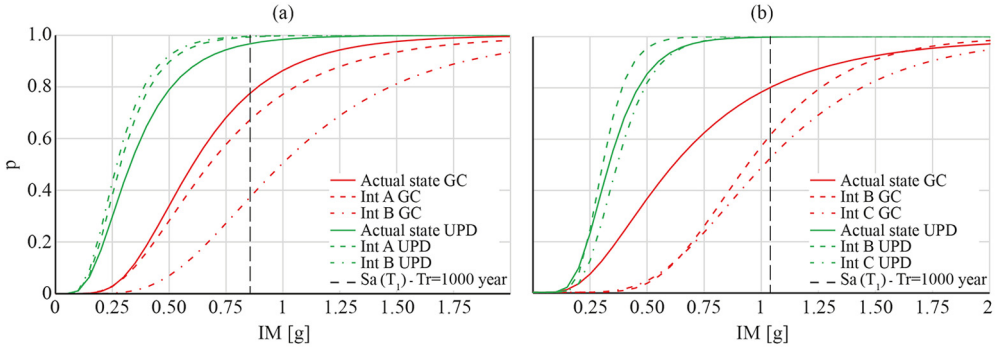

Figure 7. Fragility curves for the different configurations BLDG 1 on stiff soil (a) and soft soil (b).

7b). These curves demonstrate the actual effect of the interventions designed according to the procedures outlined in the Codes and discussed in this study. In the graphs, the GC fragility curves are shown in red, while the UPD are in green. The continuous line represents the as-built configuration of the building, while the dashed lines depict the two retrofitted scenarios. From Figure 7, it is notable that:

- Generally, all strengthening scenarios enhance the seismic performance of the building with respect to the GC. However, for soft soil, both types of interventions have a similar effect (with the two dashed fragility curves nearly overlapping). In contrast, for stiff soil, Type B intervention appears to be more effective than Type A.
- Conversely, the strengthening scenarios do not improve UPD performance. The dashed fragility curves are shifted to the left, indicating reduced performance. This outcome may be attributed to the inherent definition of UPD, based on the spread of damage, as described more in detail in Section "Discussion of the results and future developments."

To quantify the effects of the different retrofitting scenarios, the probability of exceeding the two performance states was computed by intersecting the fragility curves with the IM associated with a return period of 1000 years (indicated by the black vertical line in Figure 7). The latter is consistent with the return period associated with the seismic response spectrum used in the NLSA. For the GC limit state on stiff soil, the probability of exceedance for the as-built state is slightly higher than for Type A intervention, and significantly higher than for Type B intervention, highlighting the greater effectiveness of the latter. Interestingly, this difference in effectiveness was not fully captured by the safety indexes (α) obtained from the NLSA conducted according to the Code procedure. For these analyses, both types of interventions were considered equally effective, with α values of 0.69 for the as-built state, 0.84 for Type A intervention, and 1.05 for Type B intervention (see Table 3).

Application of the procedure to BLDG 2

This section illustrates the application of the proposed procedure described in Section "Adopted procedure for the seismic assessment and the design of strengthening interventions" to the second case study, the 3-story URM building inspired by the Pizzoli town hall near L'Aquila (BLDG 2).

Code-based assessment of the as-built configuration and design of retrofit interventions

Figure 8 shows the 3D view of the numerical EF model (Figure 8a) and a standard floor plan (Figure 8b). On the plan, the unloading paths (80% in the main direction and 20% in the secondary direction) are indicated as well as the data of stiffness used for the equivalent diaphragms, namely the shear modulus (G_D), and the Young's moduli in the main (E_{1D}) and secondary (E_{2D}) directions. These assumptions are compatible with the rigid floors present in the building. As for BLDG 1, the wall mesh was defined according to the criteria outlined by Lagomarsino et al. (2013), which were automatically applied using the 3muri software. After the mesh definition, NLSAs were performed using the two load patterns described in the first case study, applied alternatively along the two orthogonal directions. These analyses were conducted considering both stiff and soft soil conditions.

Following the same strategy described for BLDG 1, three types of strengthening interventions were designed:

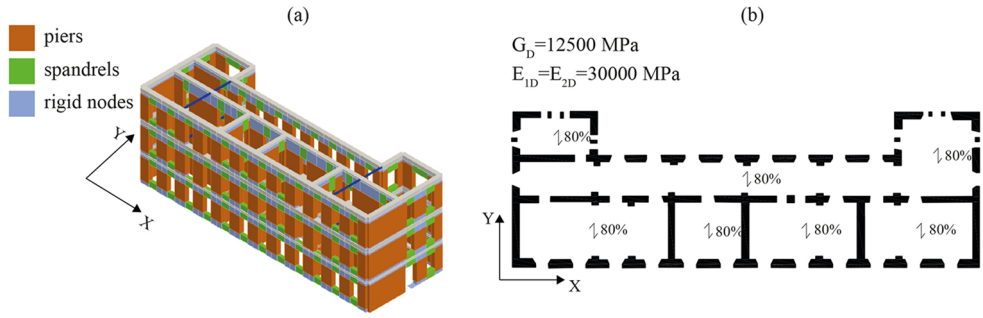

Figure 8. (a) 3D view of the geometrical model of BLDG2 and (b) floor plan of the building.

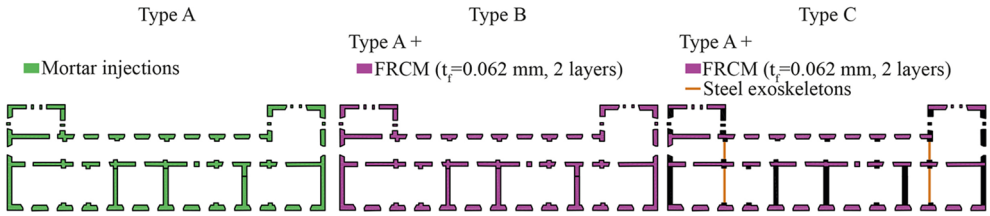

Figure 9. Interventions designed for BLDG 2 identified on the plan.

- Type A intervention: this involves mortar injections in all masonry piers. With this intervention, the safety index exceeded 1 for the L'Aquila site with stiff soil condition.
- Type B intervention: this includes mortar injections in all masonry piers and spandrels, along with the addition of two layers of FRCM (thickness t_f = 0.062 mm, tensile modulus of elasticity E_f = 60,000 GPa, ultimate deformation ε_{fk} = 3%) on the piers in both the X and Y-directions. This intervention achieved a safety index greater than 0.8 for soft soil.
- Type C intervention: this consists of mortar injections in all masonry piers and spandrels, the application of two layers of FRCM on the piers in the X-direction, and the installation of steel exoskeletons along two alignments in the Y-direction (see Figure 11). This retrofitting strategy resulted in a safety index higher than 1 in all analyses, even for the building on soft soil.

These interventions are identified in the plan in Figure 9.

Table 5 summarizes the strengthening interventions designed for BLDG 2 following NTC (2018), while Table 6 presents the safety indexes (α) obtained from the NLSA. Similar to BLDG 1, the table includes the minimum and maximum values for different load distribution patterns (i.e. proportional to masses and proportional to the product of masses and heights) across various configurations (current state and different retrofitted scenarios) and soil types (stiff or soft). The color legend indicates whether α is higher than 1 (green), higher than 0.8 (orange), or lower than 0.8 (red). As for BLDG1, the safety indexes correspond to the near-collapse limit states defined by NTC (2018).

Table 5. Summary of the strengthening interventions designed for BLDG 2 according to NTC (2018)

Site category	Objective 1 $\alpha>0.8$	Objective 2 $\alpha>1$
Stiff soil	/	Type A intervention
Soft soil	Type B intervention	Type C intervention

Table 6. Summary of safety indexes obtained for BLDG 2 from the NLSA in the different configurations considered (as-built and retrofitted configurations), varying the soils (stiff and soft)

Site category		As-built				Type A intervention	
Stiff soil		Min	Max			Min	Max
	Uniform X	1.26	1.29			1.22	1.35
	Static Force X	1.09	1.11			1.10	1.12
	Uniform Y	0.69	0.83			1.00	1.95
	Static Force Y	0.54	0.92			1.00	1.36
		As-built		Type B intervention		Type C intervention	
Soft soil		Min	Max	Min	Max	Min	Max
	Uniform X	0.74	0.89	1.31	1.37	1.35	1.38
	Static Force X	0.70	0.72	1.09	1.12	1.10	1.13
	Uniform Y	0.39	0.47	0.83	1.01	1.19	1.35
	Static Force Y	0.30	0.51	0.80	0.96	1.00	1.11

The color legend indicates whether α is higher than 1 (green), higher than 0.8 (orange), or lower than 0.8 (red).

Figure 10 shows the 24 pushover curves obtained from the NLSA performed with the 3muri software in the code-based assessment phase. The graphs indicate that the Y-direction is more vulnerable, exhibiting a lower maximum base shear across all examined configurations. This vulnerability is due to the limited number of walls and the presence of many openings in the Y-direction (see Figure 2b), compared to the X-direction. In addition, the designed strengthening interventions improve both strength and stiffness, reducing the elastic first period from 0.48 s in the as-built configuration to a range of 0.34–0.39 s in the retrofitted configurations (these values were obtained from the modal analysis). Furthermore, Type B and Type C interventions also enhance the maximum displacement capacity.

While the modeling strategies for all other interventions have already been described for the previous case study in Section "Code-based assessment of the as-built configuration and design of retrofit interventions," the following details explain how the steel exoskeletons in the Type C intervention were implemented in the numerical model of BLDG 2. Figure 11 shows the geometry of the steel exoskeletons, their placement in plan, and the cyclic pushover curves, distinguishing between the shear-displacement curve of the masonry wall and those of the two exoskeletons. The frames were designed to ensure the usability of the internal spaces; therefore, the X-shaped frame was placed only to separate two adjacent rooms, while the V-shaped frame did not obstruct the hallway. The exoskeletons comprise X-braces with active tensile diagonals and V-braces with dissipative elements. Since masonry buildings are inherently stiff, attempting to utilize the dissipative capacity of the braced frames is unnecessary. Thus, the exoskeletons were designed to

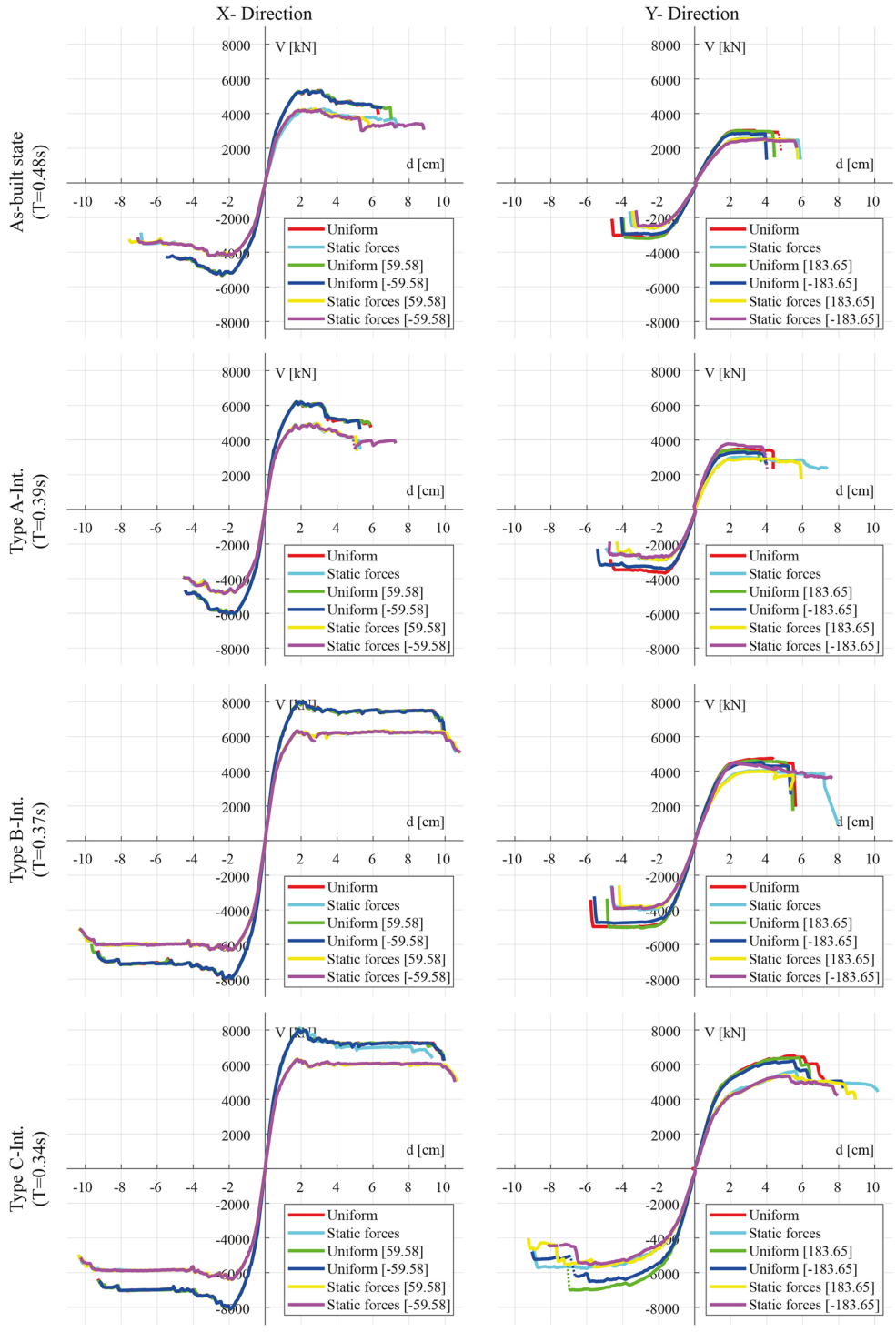

Figure 10. Pushover curves obtained from the NLSA with the 3muri software: as-built configuration and different strengthening interventions designed for BLDG 2.

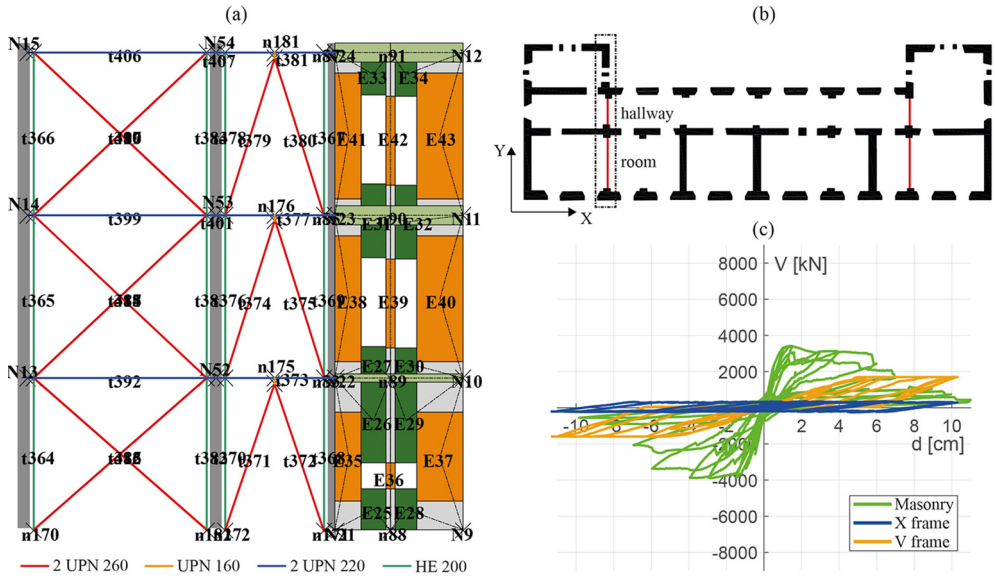

Figure 11. (a) Geometry of the steel exoskeletons designed in Type C intervention; (b) Identification of the exoskeletons in plan; and (c) Cyclic pushover curves of masonry wall, X-shaped, and V-shaped exoskeletons.

remain within the elastic range, with plasticization of the first elements occurring only after the masonry's base shear starts to decrease at the post-peak stage (Figure 11c). For the V-shaped exoskeleton, the dissipative "fuse" element was designed to experiences yielding before the buckling of the compressed brace.

Regarding the geometry and dimensions of the elements, 2UPN 260 ("C" cross-shape with height h = 260 mm, base b = 90 mm, area A = 96.60 cm^2, Mass moment of inertia J_x = 9648 cm^4 and J_y = 1172.02 cm^4) was selected for the diagonals of the X-shaped frame and the braces of the V-shaped frame, while the dissipative "fuse" consists of a UPN160 ("C" cross-shape with h = 160 mm, b = 65 mm, A = 48 cm^2, J_x = 1850 cm^4 and J_y = 332.71 cm^4), 15 cm high. All the beams are 2UPN 220 ("C" cross-shape with h = 220 mm, b = 80 mm, A = 74.80 cm^2, J_x = 5382 cm^4 and J_y = 734.55 cm^4), while the pillars are HE200 ("H" cross-shape with h = 190 mm, b = 200 mm, A = 53.83 cm^2, J_x = 3692 cm^4 and J_y = 1336 cm^4) sections. Finally, the exoskeletons were separated from the existing masonry wall using 2UPN 220 profiles.

Results of the seismic assessment

Table 7 presents the parameters used for the structural elements during the assessment phase for BLDG 2.

Figure 12 illustrates the fragility curves computed using the R2R software with the assumption of either stiff or soft soil conditions. From this figure, it is notable that:

- Similar to BLDG 1, all strengthening scenarios enhance the building's seismic performance for the GC limit state.

Table 7. Parameters adopted for piers and spandrels (in brackets) in the piece-wise linear constitutive law for BLDG 2

	SHEAR		*FLEXURAL*	
	Drift [%]	Residual strength [%]	Drift [%]	Residual strength [%]
DL3	0.45 (*)	60 (60)	0.60 (0.60)	100 (100)
DL4	0.73 (0.40)	20 (60)	0.90 (0.80)	85 (60)
DL5	2.00 (1.50)	0 (0)	2.00 (1.80)	0 (0)

*Defined starting from drift corresponding to the yielding point of the element and assuming a ductility factor equal to 4.

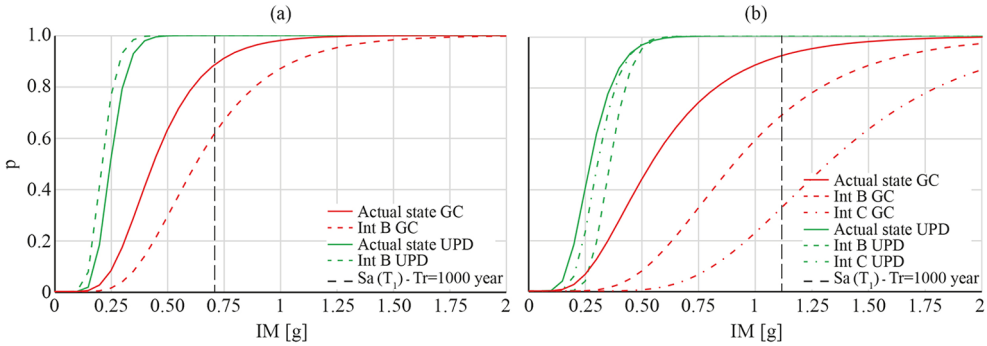

Figure 12. Fragility curves for the different configurations of BLDG 2 on stiff soil (a) and soft subsoil (b).

- However, the impact of the strengthening scenarios on the UPD performance is not beneficial for stiff soil, as indicated by the fragility curves shifting to the left.

To quantify the effects of the various retrofitting scenarios, the probability of exceedance of the two performance states was calculated by intersecting the fragility curves with the IM associated with a return period of 1000 years (indicated by the black vertical line in Figure 12). Regarding the GC limit state for both soil types, the probability of the as-built condition is higher than that of all retrofitted configurations, demonstrating the effectiveness of the strengthening interventions.

Discussion of the results and future developments

Despite the differences in masonry typologies and configurations, the transversal direction was the most vulnerable for both case studies, as only a few walls are oriented in that direction. The minimum safety index values determined via NLSA before the strengthening interventions were 0.69 (stiff soil) and 0.46 (soft soil) for BLDG 1, and 0.54 (stiff soil) and 0.30 (soft soil) for BLDG 2. As expected, the nonlinear static analysis indicates that the structural performance on soft soil is worse, because of the more demanding seismic response spectrum. Various strengthening techniques were designed and implemented in the numerical models to improve the seismic performance, up to a minimum level ($\alpha > 0.8$) and to the full verification ($\alpha > 1$), selecting interventions that were gradually more invasive. The pushover curves obtained through NLSA before and after the strengthening interventions are compared in Figure 13 for both case studies.

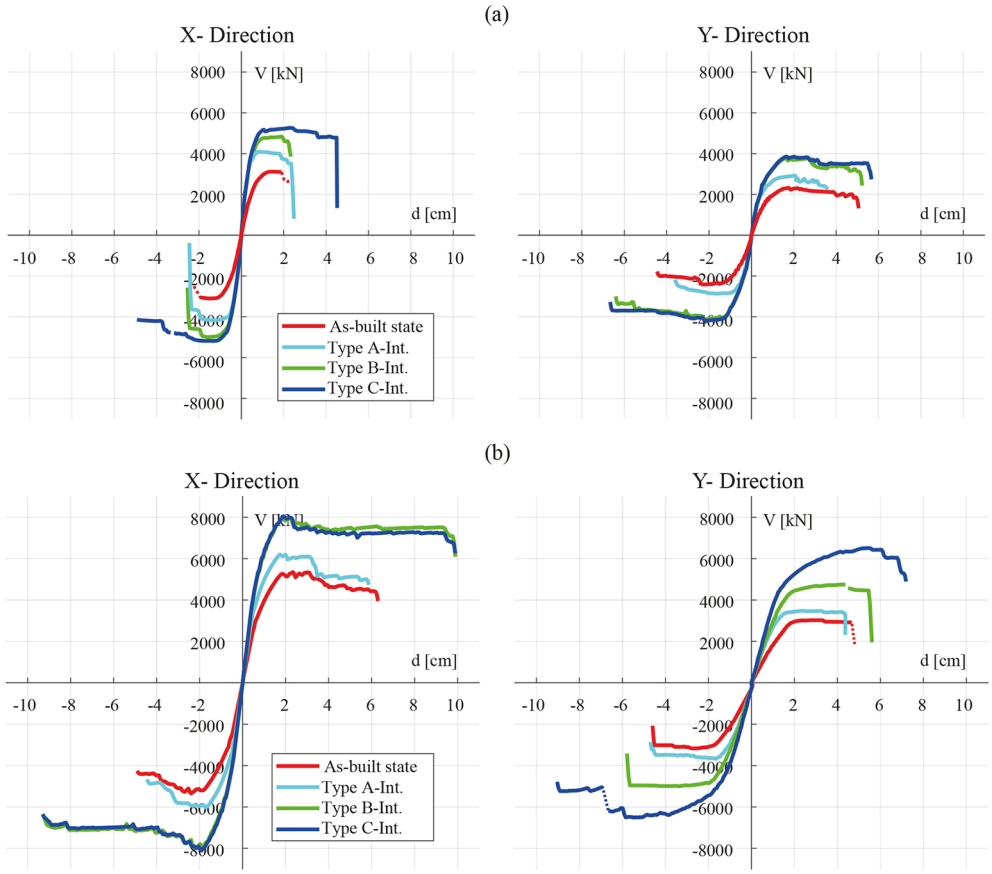

Figure 13. Pushover curves by NLSA (uniform load pattern) before and after strengthening interventions for BLDG 1 (a) and BLDG 2 (b).

As shown, all selected interventions increased stiffness. In addition, the interventions can either increase strength and displacement capacity (those with FRCM) or only increase strength (all other interventions). In the case of BLDG 1, the selected retrofitting solutions allowed the building to achieve higher safety levels by substantially improving only the performance of the masonry walls. In contrast, for BLDG 2, increasing the mechanical properties of the masonry enabled the building to achieve a safety index greater than one on stiff soil only. To achieve similar results on soft soil, however, additional resisting elements were necessary to overcome the vulnerability inherent in the plan layout.

An interesting finding from applying the procedure to both case studies is that the nonlinear static approach predicts a more step-by-step increase in performance as the intervention type progresses from Type A to Type C, regardless of the assumed soil. In contrast, the results of the NLDA used to compute the fragility curves showed that, while the benefits of the retrofitting solutions on GC are evident for both buildings and soils, the increase in performance may be less gradual, as in BLDG 1 on stiff soil. Furthermore, according to the results of NLDA, different interventions may have a similar impact on the structural performance. This is the case for the strengthening interventions designed for BLDG 1 on soft soil, where a limited variation in the fragility curves was observed when implementing

FRCM only in the internal walls (as in Type B interventions) or also in the perimeter walls (as in Type C interventions). These differences can be attributed to the limitations of the static procedure, which does not explicitly account for specific features of the seismic input that also influence the analysis results, as performance is calculated by comparing the capacity curve with a conventional seismic response spectrum. At the same time, retrofitting solutions that enhance the building's performance at the ultimate limit state could worsen it under lower damage conditions. This was evident from the analysis of the two case studies, where the fragility curves for the UPD generally showed a slightly lower performance after the interventions. This may occur because the UPD in this study is defined based on damage diffusion. Therefore, an intervention that causes more widespread damage may promote the attainment of UPD. Furthermore, while NLSA tends to localize damage due to the use of fixed loading patterns, NLDA involves the contribution of higher modes. Although an assessment based on NLDA is more accurate and better represents the actual structural behavior during an earthquake, one potential drawback is that the results are very sensitive to record-to-record variability.

In light of these considerations, the primary implication of the proposed procedure is the synergistic use of both approaches to overcome the limitations of each methodology. The nonlinear static approach serves as a practical tool for quickly assessing a building's safety with reasonable computational effort. It also allows practitioners to easily implement various retrofitting strategies by providing initial insights into how these strategies impact the building's overall behavior. However, the use of NLDA is recommended for a more accurate representation of the building's dynamic behavior, as the specific features of the records may influence its response. This approach can increase practitioners' awareness and enable them to predict the actual performance improvement and potential change in response. As a result, practitioners can make informed decisions when selecting the retrofitting options, best suited to the building.

A key challenge in obtaining reliable results is selecting the most appropriate modeling strategy, considering the specific building's characteristics and the relevant expected responses. In the examined case studies, where a box-like behavior prevails, an EF modeling strategy was adopted, which only accounts for the in-plane behavior of the masonry walls. However, as a potential future development of this study, the results could be expanded to include an analysis of out-of-plane mechanisms. To achieve this, it would be necessary to identify all possible local mechanisms, and NLDA should be performed using the time histories derived from the global EF model. These time histories are usually modified by the building's dynamic features inducing an amplified seismic input acting at the base of the local mechanism (Degli Abbati et al., 2022b). Finally, the results should be processed to generate fragility curves, first for individual failure mechanisms and then for the overall combined behavior under various performance conditions. This can be done using a procedure like the one proposed by Angiolilli et al. (2021), who presented a case study where the fragility at the ultimate limit states is affected by the interactions between in-plane and out-plane failures, while in-plane response mainly governs seismic response at the damage limit state.

Conclusion

This article presents a procedure for deriving fragility curves to assess and compare the effectiveness of retrofitting strategies for unreinforced masonry (URM) buildings. The procedure is intended as a valuable tool to support practitioners: first, in understanding

the dynamic behavior of structures possibly modified by strengthening interventions, and second, in selecting optimal retrofitting solutions. The procedure uses a reliable numerical model of the building, capable of capturing its nonlinear response. The numerical model must consider the building's specific features and expected responses. In the examined case studies, an equivalent frame (EF) modeling strategy was used, which only considers the in-plane response of walls. This limitation should be overcome in the future development of this study by also including the analysis of out-of-plane mechanisms. After the numerical model definition, the procedure is carried out in two stages. In the "code-based assessment" phase, the seismic assessment of the building in the as-built configuration is performed via nonlinear static analyses (NLSA) to determine whether improvements are necessary. In addition, various strengthening interventions are designed and implemented within the numerical model to quantify their effect on structural performance. This stage aligns with the methods typically employed by practitioners when assessing existing buildings, utilizing the techniques and assumptions prescribed by relevant codes and quantifying their implications for safety assessments. In the "assessment phase," the actual effects of the designed strengthening interventions are evaluated using nonlinear dynamic analyses (NLDA), which are then compared with the results of equivalent static procedures. To this aim, appropriate constitutive laws are implemented in the numerical model, and fragility curves are derived based on the output from the NLDA.

To demonstrate reliability of the procedure, it is applied to two 3-story URM buildings modeled after existing structures and selected for their distinct morphological features. In both cases, the buildings exhibit a more vulnerable direction; however, this characteristic is more pronounced in BLDG 2, which has an elongated plan with few walls and many openings in the Y-direction. The NLSA initially performed on the equivalent frame nonlinear model of the buildings highlighted the necessity of enhancing their seismic performance by designing and implementing various retrofitting strategies in the numerical models to achieve a safety index greater than 1 or 0.8, depending on two different site categories (stiff and soft soils). The NLDA conducted on both the as-built and retrofitted configurations allowed the authors to quantify the actual impact of the selected strengthening interventions by comparing the resulting fragility curves for two different performance states: global collapse and usability-preventing damage. The results of this study indicated that, for the two selected case studies, the code-prescribed procedures commonly used by practitioners serve as a practice-oriented tool to quantify structural safety and design strengthening interventions, provided that appropriate modeling strategies and assumptions are implemented in the numerical model. However, these procedures may not fully capture the true effects of the designed strengthening interventions on the buildings' seismic response. For this reason, the use of NLDA is recommended to increase practitioners' awareness of the actual dynamic behavior of the buildings and to select optimal retrofitting solutions. Finally, the proposed procedure based on the derivation of fragility curves appears promising, as it effectively quantifies the probability of exceeding the target performance states in both the as-built and retrofitted configurations, providing valuable insights for identifying the most effective retrofitting solutions.

Acknowledgments

The study presented in this article was developed within the activities of the 2022–2024 ReLUIS-DPC project research programs (namely, the RINTC project), funded by the Presidenza del Consiglio dei Ministri—Dipartimento della Protezione Civile (DPC).

Author contributions

SDA and AB: Analysis, Data curation, Visualization, Writing – original draft; AR: Analysis, investigation; SL: Supervision, Writing – review & editing. All authors read and approved the final manuscript.

Declaration of conflicting interests

The author(s) declared no potential conflicts of interest with respect to the research, authorship, and/or publication of this article.

Funding

The author(s) received no financial support for the research, authorship, and/or publication of this article.

ORCID iDs

Stefania Degli Abbati https://orcid.org/0000-0001-9991-8599
Sergio Lagomarsino https://orcid.org/0000-0002-6597-3474

Data and Resources

The folder containing the data used in this study can be downloaded from: https://doi.org/10.5281/zenodo.15294542. It includes the accelerograms used for the nonlinear dynamic analyses, which were shared with the research units involved in the activities carried out within the framework of the 2022–2024 RINTC project (Iervolino et al., 2023b), as well as the numerical models of the two examined case studies.

References

Angiolilli M, Lagomarsino S, Cattari S and Degli Abbati S (2021) Seismic fragility assessment of existing masonry buildings in aggregate. *Engineering Structures* 247: 113218.

ASCE/SEI 41-23 (2023) Seismic evaluation retrofit of existing buildings. Reston, VA: ASCE.

Augenti N and Parisi F (2010) Learning from construction failures due to the 2009 L'Aquila, Italy, earthquake. *Journal of Performance of Constructed Facilities* 24: 536–555.

Augenti N (2006) Seismic behavior of irregular masonry walls In: *Proceedings of the 1st European conference on earthquake engineering seismology*, Geneva, 3–8 September.

Baraschino R, Baltzopoulos G and Iervolino I (2020) R2R-EU: Software for fragility fitting and evaluation of estimation uncertainty in seismic risk analysis. *Soil Dynamics and Earthquake Engineering* 132: 106093.

Beyer K and Mangalathu S (2014) Numerical study on the peak strength of masonry spandrels with arches. *Journal of Earthquake Engineering* 18(2): 169–186.

Cattari S and Lagomarsino S (2013) Masonry structures. In: Sullivan TJ and Calvi GM (eds) *Developments in the field of displacement based seismic assessment*. Pavia: IUSS Press, pp. 151–200; Eucentre, pp. 524.

Cattari S, Camilletti D, D'Altri AM and Lagomarsino S (2021) On the use of continuum finite element and equivalent frame models for the seismic assessment of masonry walls. *Journal of Building Engineering* 43: 102519.

Cattari S, Degli Abbati S, Ferretti D, Lagomarsino S, Ottonelli D, Rossi M and Tralli A (2012) The seismic behaviour of ancient masonry buildings after the earthquake in Emilia (Italy) on May 20th and 29th, 2012. *Ingegneria Sismica* 29: 87–119.

CEN EN 1998-1 (2004) Eurocode 8: Design of structures for earthquake resistance—Part 1: General rules, seismic actions and rules for buildings. Brussels: CEN.

CNR-DT (215/2018) (2018) Guide for the design and construction of externally bonded fibre reinforced inorganic matrix systems for strengthening existing structures. *The National Research Council*, 30 June, Roma.

D'Altri AM, Sarhosis V, Milani G, Rots J, Cattari S, Lagomarsino S, Sacco E, Tralli A, Castellazzi G and de Miranda S (2020) Modeling strategies for the computational analysis of unreinforced masonry structures: Review and classification. *Archives of Computational Methods in Engineering* 27: 1153–1185.

D'Ayala DF and Paganoni S (2011) Assessment and analysis of damage in L'Aquila historic city centre after 6th April 2009. *Bulletin of Earthquake Engineering* 9: 81–104.

Degli Abbati S, Cattari S and Lagomarsino S (2022b) Validation of a practice-oriented floor spectra formulation through actual data from the 2016/2017 Central Italy earthquake. *Bulletin of Earthquake Engineering* 20: 7477–7511.

Degli Abbati S, Morandi P, Cattari S and Spacone E (2022a) On the reliability of the equivalent frame models: The case study of the permanently monitored Pizzoli's town hall. *Bulletin of Earthquake Engineering* 20: 2187–2217.

Dolce M (1991) Schematizzazione e modellazione degli edifici in muratura soggetti ad azioni simiche. *L'industria Delle Costruzioni* 25(242): 44–57 (in Italian).

Fajfar P (1999) Capacity spectrum method based on inelastic demand spectra. *Earthquake Engineering & Structural Dynamics* 28(9): 979–993.

Freeman SA (1998) The capacity spectrum method as a tool for seismic design. In: *11th European Conference of Earthquake Engineering*, Paris, 6–11 September 1998.

Gkournelos PD, Triantafillou TC and Bournas DA (2022) Seismic upgrading of existing masonry structures: A state-of-the-art review. *Soil Dynamics and Earthquake Engineering* 161: 107428.

Iervolino I (2017) Assessing uncertainty in estimation of seismic response for PBEE. *Earthquake Engineering & Structural Dynamics* 46: 1711–1723.

Iervolino I, Baraschino R and Spillatura A (2023a) Evolution of seismic reliability of code-conforming Italian buildings. *Journal of Earthquake Engineering*: 27: 1740–1768.

Iervolino I, Baraschino R, Belleri A, Cardone D, Della Corte G, Franchin P, Lagomarsino S, Magliulo G, Marchi A and Penna A (2023b) Seismic fragility of Italian code-conforming buildings by multi-stripe dynamic analysis of three-dimensional structural models. *Journal of Earthquake Engineering* 27: 4415–4448.

Iervolino I, Spillatura A and Bazzurro P (2018) Seismic reliability of code-conforming Italian buildings. *Journal of Earthquake Engineering* 22(suppl. 2): 5–27.

Jalayer F, Ebrahimian H and Miano A (2021) Record-to-record variability and code-compatible seismic safety-checking with limited number of records. *Bulletin of Earthquake Engineering* 19: 6361–6396.

Lagomarsino S and Cattari S (2015) Seismic performance of historical masonry structures through pushover and nonlinear dynamic analyses. *Perspectives on European Earthquake Engineering and Seismology* 2: 265–292.

Lagomarsino S, Cattari S, Angiolilli M, Bracchi S, Rota M and Penna A (2023) Modelling and seismic response analysis of existing URM structures. Part 2: Archetypes of Italian historical buildings. *Journal of Earthquake Engineering* 27: 1849–1874.

Lagomarsino S, Penna A, Galasco A and Cattari S (2013) TREMURI program: An equivalent frame model for the nonlinear seismic analysis of masonry buildings. *Engineering Structures* 56: 1787–1799.

Lin T, Haselton CB and Baker JW (2013) Conditional spectrum-based ground motion selection. Part I: Hazard consistency for risk-based assessments. *Earthquake Engineering & Structural Dynamics* 42: 1847–1865.

Marino S, Cattari S and Lagomarsino S (2019) Are the nonlinear static procedures feasible for the seismic assessment of irregular existing masonry buildings? *Engineering Structures* 200: 109700.

MIT (2019) Istruzioni per l'applicazione dell'aggiornamento delle norme tecniche per le costruzioni di cui al Decreto Ministeriale 17 Gennaio 2018. *Ministry of Infrastructures and Transportation*, G.U. S.O. N.35 of 11 February 2019 (in Italian).

Moon FL, Yi T, Leon RT and Kahn LF (2006) Recommendations for seismic evaluation and retrofit of low-rise URM structures. *Journal of Structural Engineering* 132(5): 663–672.

Mouyiannou A, Rota M, Penna A and Magenes G (2014) Identification of suitable limit states from nonlinear dynamic analyses of masonry structures. *Journal of Earthquake Engineering* 18(2): 231–263.

NTC (2018) Norme Tecniche per le Costruzioni. *DM 17/01/2018, Italian Ministry of Infrastructure and Transportation*, G.U. N. 42 of 20 February 2018, Rome (in Italian).

Ottonelli D, Manzini CF, Marano C, Cordasco EA and Cattari S (2021) A comparative study on a complex URM building: Part I–sensitivity of the seismic response to different modelling options in the equivalent frame models. *Bulletin of Earthquake Engineering* 20: 2115–2158.

Penna A, Morandi P, Rota M, Manzini CF, Da Porto F and Magenes G (2014) Performance of masonry buildings during the Emilia 2012 earthquake. *Bulletin of Earthquake Engineering* 12: 2255–2273.

Sorrentino L, Cattari S, da Porto F, Magenes G and Penna A (2019) Seismic behaviour of ordinary masonry buildings during the 2016 central Italy earthquakes. *Bulletin of Earthquake Engineering* 17(10): 5583–5607.

Spence R and D'Ayala D (1999) Damage assessment and analysis of the 1997 Umbria-Marche earthquakes. *Structural Engineering International* 9: 229–233.

Vanin F, Zaganelli D, Penna A and Beyer K (2017) Estimates for the stiffness, strength and drift capacity of stone masonry walls based on 123 quasi-static cyclic tests reported in the literature. *Bulletin of Earthquake Engineering* 15: 5435–5479.